Edge Enhanced and Nonlocal Sparse Representation for Image Denoising

QIAN WANG
Tianjin University
Department of Mathematics
300072, Tianjin
P. R. China
wangqian23@tju.edu.cn

PING WANG
Tianjin University
Department of Mathematics
300072, Tianjin
P. R. China
wang_ping@tju.edu.cn

YUWEI ZANG*
Tianjin Tendbeyond S&T Development Co.,Ltd
300072, Tianjin
P. R. China
zangyw@tendbeyond.com

Abstract: Sparse representation and nonlocal self-similarity play an important role and show better results in image denoising. However, the methods based on sparse representation or nonlocal self-similarity tend to smooth the image edge structures or generate some artifacts. To improve the performance of image denoising, in this paper we propose an edge enhanced and nonlocal sparse representation (ENSR) model which combines Sobel edge detection results, local sparsity and nonlocal self-similarity. We use the iterative shrinkage algorithm to solve the l_1-regularized ENSR minimization problem. The experimental results show that ENSR can better preserve the edge structure and achieve a competitive PSNR performance compared with some existing methods.

Key–Words: Image denoising, Sparse representation, Sobel operator, Nonlocal self-similarity.

1 Introduction

Image denoising is an important part in the field of image processing and low level vision. The goal is to recover the latent clean image x from a noisy observation y, and the denoising problem can be formulated as

$$y = x + v, \tag{1}$$

where v is additive noise. With the rapid development of compressed sensing, many researchers used sparse coding to solve image denoising problems [1–9]. Generally, the sparse representation model assumes that a signal $x \in \Re^2$ can be represented by $x \approx D\alpha$ where $D \in \Re^{n\times m}(n < m)$ is a dictionary, and most entries of coefficient α are zero or close to zero. Sparse representation using KSVD [1–3] to learn an over-complete dictionary is a powerful method for image denoising. Mairal *et al*.[4] proposed a method for image restoration which unified sparse coding and the self-similarities of natural images. [6, 7] exploited the merits of the wavelet transform and sparse coding to learn multi-scale dictionaries. Moreover, principle component analysis(PCA) [8, 9] was also employed as a dictionary learning method.

In recent years, the regularization terms in image denoising problems usually fall into two categories: local vs. nonlocal. However, nonlocal image representation shows more remarkable performances - e.g., block-matching and 3-D filtering (BM3D) [10], learned simultaneous sparse coding (LSSC) [4], nonlocally centralized sparse representation (NCSR) [5], weighted nuclear norm minimization (WNNM) [11]. In addition, the methods associated with the nonlocal self-similarity and sparse coding have received increasingly more attention [4, 5, 11] which have broadly encouraging results in both visual perception quality and quantitative measure. Moreover, Talebi *et al*.[12] proposed a global denoising filter where every single pixel was estimated from all pixels in the image. Although many denoising algorithms achieve great success, they often fail to preserve the edge structure. Based on the above facts, we propose an edge enhanced and nonlocal sparse representation model for image denoising. We aim to enhance the edge structures while removing noise.

Edge information is the most basic feature of an image which contains important structure information. [13] and [14] proposed some methods for image denoising and edge enhancement based on the wavelet transform. Gao *et al*. [15] proposed an edge detection method which combined soft-threshold wavelet denoising and Sobel edge detection operator. Qiu *et al*. [16] proposed an image denoising method which could preserve edge structure partly. In this paper, we choose Sobel operator to do edge detection which has certain smoothing effect on the noise in images. We add edge enhanced regularization term in the framework of nonlocally sparse coding to increase the quali-

*corresponding author

ty of visual perception. The edge enhanced regularization term avoids the problem of over-smoothed edge. The main contribution of this paper is a better balance between the enhanced regularization term and the sparse coding. To the best of our knowledge, this has never been done in any previous works. The basic idea of our ENSR is to treat local sparsity, non-local self-similarity and edge information as peers and incorporate them into a unified variational framework.

The rest of the paper is organized as follows. Section 2 describes the edge enhanced and nonlocal sparse representation for image denoising model and its algorithm. Section 3 presents experimental results and Section 4 includes some concluding remarks.

2 The Edge Enhanced Image Denoising

We consider a patch-based image denoising method and the noise is additive zero-mean white Gaussian noise with variance σ^2. Following the mathematical notation as [1], $x \in \Re^2$ is an image vector, $x_i = R_i x$ where x_i represents the i-th image patch of size $\sqrt{n} \times \sqrt{n}$, $i = 1, 2, \ldots, N$, and R_i is the matrix which extracts the image patch x_i from x. Given a dictionary D, we can use D to sparsely represent $x_i = D\alpha_i$ where α_i is a sparse coding vector. The whole image x can be reconstructed by a straightforward least-square solution which can be formulated as follows [1]:

$$x = D \circ \alpha \triangleq (\sum_{i=1}^{N} R_i^T R_i)^{-1} \sum_{i=1}^{N} R_i^T D\alpha_i, \qquad (2)$$

where α is the concatenation of all α_i.

The performance of image denoising depends on the choice of reconstruction item and regularization term. In recent years, the mainstream image denoising method based on sparse coding is usually modeled as

$$\hat{\alpha} = \arg\min_{\alpha} \{\|y - D\alpha\|_2^2 + \lambda \cdot R(\alpha)\}, \qquad (3)$$

where λ is a positive parameter. In this paper, we join an edge enhanced term in (3).

2.1 Sobel Operator

Compared with other edge detection algorithms, Sobel operator has some smoothing effects when it encounters the random noise in images, and the edge obtained by Sobel operator is bright and thick[15]. In this paper, we use Sobel operator to do the edge detection because it is insensitive to noise compared with other operators.

Figure 1: Edge detection results of Lena, Fingerprint, and Hill.

Its digital gradient approximation equations are as follows:

$$G_x = \{f(x+1, y-1) + 2f(x+1, y) + f(x+1, y+1)\} - \{f(x-1, y-1) + 2f(x-1, y) + f(x-1, y+1)\}, \qquad (4)$$

$$G_y = \{f(x-1, y+1) + 2f(x, y+1) + f(x+1, y+1)\} - \{f(x-1, y-1) + 2f(x, y-1) + f(x+1, y-1)\}, \qquad (5)$$

where G_x and G_y represent the X direction and Y direction respectively. The magnitude of its gradient is calculated according to $g(x, y) = \sqrt{G_x^2 + G_y^2}$. We use a threshold method to get the edge. Sobel operator can also be expressed through its convolution template operators

$$T_x = \begin{bmatrix} -1 & 0 & 1 \\ -2 & 0 & 2 \\ -1 & 0 & 1 \end{bmatrix}, \qquad T_y = \begin{bmatrix} -1 & -2 & -1 \\ 0 & 0 & 0 \\ 1 & 2 & 1 \end{bmatrix}.$$

Sobel edge detection results can be displayed in the form of image as shown in Fig.1. Here we define a linear transformation, $g(\alpha; A) = A\alpha$, which can guarantee $e = A\alpha$, where A is a transformation matrix like a dictionary and e represents the edge detection result. That is to say, edge structure can also be represented by sparse coding. We propose the following edge enhanced image denoising model:

$$\hat{\alpha} = \arg\min_{\alpha} \{\|y - D\alpha\|_2^2 + \lambda \cdot R(\alpha) + \mu\|e - A\alpha\|_2^2\}, \qquad (6)$$

where μ is a positive parameter.

2.2 The Denoising Model

To make the edge enhanced denoising model more effective, a good regularization term $R(\alpha)$ is crucial. In recent years, local sparsity and nonlocal self-similarity are two priors widely used in image denoising. The regularization term in [4] and [5] which combined local sparsity and nonlocal self-similarity has brought better denoising quality. In this paper, we also adopt the sparse nonlocal regularization term like nonlocally centralized sparse representation [5] as follows:

$$R(\alpha) = \sum_i \|\alpha_i - \beta_i\|_1, \tag{7}$$

where β_i can be computed from the weighted average of $\alpha_{i,q}$ as follows:

$$\beta_i = \sum_{q \in \Omega_i} \omega_{i,q} \alpha_{i,q}, \tag{8}$$

where Ω_i is a set of patches which are similar to x_i, and $\alpha_{i,q}$ is the sparse code of the q-th nearest patch of x_i within Ω_i. $\omega_{i,q}$ is the weight defined by $\omega_{i,q} = \frac{1}{W}\exp(-\|\hat{x}_i - \hat{x}_{i,q}\|_2^2/h)$, where $\hat{x}_i = D\hat{\alpha}_i$ and $\hat{x}_{i,q} = D\hat{\alpha}_{i,q}$. h is a pre-determined scalar. Substituting Eq.(7) into Eq.(6), ENSR model can be formulated as:

$$\hat{\alpha} = \arg\min_{\alpha}\{\|y - D\alpha\|_2^2 + \mu\|e - A\alpha\|_2^2 + \lambda\sum_i \|\alpha_i - \beta_i\|_1\}. \tag{9}$$

2.3 Algorithm of ENSR

In order to solve the proposed model more effectively, Eq.(9) can be rewritten as:

$$\hat{a} = \arg\min_{\alpha}\{\left\| \begin{pmatrix} y \\ \sqrt{\mu}e \end{pmatrix} - \begin{pmatrix} D \\ \sqrt{\mu}A \end{pmatrix}\alpha \right\|_2^2 + \lambda\sum_i \|\alpha_i - \beta_i\|_1\}. \tag{10}$$

Let $y_{new} = (y^T, \sqrt{\mu}e^T)^T$, $D_{new} = (D^T, \sqrt{\mu}A^T)^T$, as the optimization method shown in [17]. Eq.(10) is equivalent to solving the following minimization problem:

$$\hat{\alpha} = \arg\min_{\alpha}\{\|y_{new} - D_{new}\alpha\|_2^2 + \lambda\sum_i \|\alpha_i - \beta_i\|_1\}. \tag{11}$$

We use the same method as that in [5] and [9] to construct the dictionary. The patches of image are clustered into K clusters, and we learn a PCA dictionary for each cluster. For a given patch, we first check which cluster it belongs to, then choose the PCA dictionary of this cluster to code it. We update α_i by the iterative shrinkage algorithm in [18]. $\alpha_i^{(l)}(j)$ is the j-th element of α_i in the l-th iteration. We can update $\alpha_i^{(l+1)}(j)$ by

$$\alpha_i^{(l+1)}(j) = S_\tau(\nu_{i,j}^{(l)} - \beta_i(j)) + \beta_i(j), \tag{12}$$

where $\nu^{(l)} = D_{new}^T(y - D_{new}\alpha^{(l)})/c + \alpha^{(l)}$, $\tau = \lambda_{i,j}/c$, and c is an auxiliary parameter. $S_\tau(\cdot)$ is soft-thresholding operator. The regularization parameter $\lambda_{i,j}$ can be computed by

$$\lambda_{i,j} = \frac{2\sqrt{2}\sigma_n^2}{\sigma_{i,j}}, \tag{13}$$

where σ_n^2 is noise variance. Let $\theta_i = \alpha_i - \beta_i$, and then $\sigma_{i,j}$ is the standard deviation of $\theta_i(j)$ which is the j-th element of θ_i (More detailed explanations can be found in [5]). When we obtain D_{new} and α, the desired dictionary $\hat{D}$ can be got from D_{new}. The reconstructed image x can be formulated as follows:

$$\hat{x} = \hat{D}\alpha. \tag{14}$$

A complete description of the ENSR algorithm is given in Algorithm 1.

Algorithm 1: Image Denoising by ENSR

1: Initialize parameters λ, μ and δ;
initialize e by Sobel edge detection result;
let $y_{new} = (y^T, \sqrt{\mu}e^T)^T$;
initialize $\hat{x}_{new} = y_{new}$.
2: Outer loop: for $i = 1, 2, \ldots, L$
(1) Update D_{new} via PCA and k-means;
(2) Inner loop: for $j = 1, 2, \ldots, J$
-update $\hat{x}_{new}$:
$\hat{x}_{new}^{(j+\frac{1}{2})} = \hat{x}_{new}^{(j)} + \delta(y - \hat{x}_{new}^{(j)})$,
where δ is the pre-determined constant;
-update $\nu^{(l)}$:
$\nu^{(l)} = D_{new}^T \hat{x}_{new}^{(j+\frac{1}{2})}$;
-update $a_i^{(l+1)}$ using Eq.(12);
-update $\lambda_{i,j}$ by Eq.(13).
3: Extract $\hat{D}$ from D_{new},
and image estimate $\hat{x} = \hat{D}\alpha$.

3 Experiment

In this section, our ENSR method is evaluated and compared with several image denoising methods, including block-matching and 3-D filtering (BM3D)

Figure 2: The twelve images for test. From left to right and top to bottom: Lena, Monarch, Barbara, Boat, Cameraman, Couple, Fingerprint, Hill, House, Man, Peppers, Straw.

[10], the learned simultaneous sparse coding (LSSC) [4], and the nonlocally centralized sparse representation (NCSR) [5]. In subsection 3.1, we introduce the experimental parameter settings in our algorithm; in subsection 3.2, we evaluate ENSR and compare it with other methods on twelve commonly used test images as shown in Fig.2.

3.1 Parameter Setting

There are several parameters in our ENSR algorithm. The cluster number K is 55, and the constant $\delta = 0.02$. The parameter $\sqrt{\mu}$ is 0.003 when $\sigma^2 \leqslant 30$, and we set $\sqrt{\mu} = 9$ at higher noise levels to ensure good performance. We set the patch size to 6×6, 7×7, 9×9 and 8×8 for $\sigma \leq 15$, $15 < \sigma \leq 30$, $30 < \sigma \leq 50$, $50 < \sigma$, respectively. When $\sigma \leq 50$, the iteration numbers $K = 4, J = 3$, or else $K = 5, J = 3$. The process is iterated until convergence or the maximum number of iterations is reached.

3.2 Experimental Results

We conduct a lot of experiments on twelve commonly used images (Fig.2). In the experiments, the noisy image y is obtained by adding a Gaussian white noise to the original image x.

As shown in Table 1, there are PSNR results of four algorithms, and the best result for each image is in bold at each noise level. From Table 1, ENSR outperforms the other three methods including BM3D at lower noise levels. Fig.3 shows the denoising details of BM3D,LSSC,NCSR,ENSR. It can be seen that ENSR is very effective in reconstructing edge regions. When the noise level is high, BM3D has better PSNR results, but it can produce some visual artifacts as shown in Fig.4. From Fig.5, all these algorithms have a better visual quality when the noise level $\sigma = 20$. As shown in Fig.6 and Fig.7, ENSR algorithm has good effects on the texture images such as Fingerprint and Straw. This reflects the good characteristics of ENSR on edge structure and texture information. In summary, our ENSR method performs better than NCSR, and achieves better PNSR performance than BM3D and LSSC at lower noise levels.

4 Conclusion

In the paper, an edge enhanced and nonlocal sparse representation(ENSR) model is presented for image denoising. The Sobel operator is introduced in image denoising method to enhance edge structure. We use the iterative shrinkage algorithm to solve the l_1-regularized ENSR minimization problem. ENSR method combines local sparsity, nonlocal self-similarity and Sobel edge detection. The experimental results show that ENSR can better preserve the edge structure and texture information. Our proposed ENSR method outperforms NCSR, and achieves better PNSR performance than BM3D and LSSC at lower noise levels.

References:

[1] M. Aharon, M. Elad, and A. Bruckstein, K-SVD: An Algorithm for Designing Overcomplete Dictionaries for Sparse Representation, *IEEE Trans. Signal Process.* vol. 54, no.11, 2006, pp. 4311–4322.

[2] M. Elad, M. Aharon, Image Denoising Via a Sparse and Redundant Representations Over

Table 1: Denoising results(PSNR) by different methods with noise levels: 5, 10, 15, 20, 50, 100.

Images	denoising method	$\sigma = 5$	$\sigma = 10$	$\sigma = 15$	$\sigma = 20$	$\sigma = 50$	$\sigma = 100$
Lena	BM3D	38.72	**35.93**	**34.27**	**33.05**	**29.05**	25.95
	LSSC	38.68	35.83	34.14	32.88	28.95	25.96
	NCSR	38.70	35.81	34.09	32.92	28.89	25.66
	ENSR	**38.83**	35.90	34.19	33.00	29.03	**25.98**
Monarch	BM3D	38.21	34.12	31.86	30.35	**25.82**	**22.52**
	LSSC	38.53	34.48	32.15	30.58	25.59	21.82
	NCSR	38.49	34.57	32.34	30.69	25.68	22.05
	ENSR	**38.58**	**34.68**	**32.44**	**30.76**	25.71	22.23
Barbara	BM3D	38.31	34.98	**33.11**	**31.78**	**27.23**	**23.62**
	LSSC	38.44	34.95	32.96	31.53	27.13	23.56
	NCSR	38.36	34.98	33.02	31.72	27.10	23.30
	ENSR	**38.47**	**35.06**	**33.11**	31.77	26.85	23.22
Boat	BM3D	37.28	33.92	32.14	**30.88**	**26.78**	**23.97**
	LSSC	37.34	**33.99**	**32.17**	30.87	26.76	23.94
	NCSR	37.35	33.90	32.03	30.74	26.60	23.64
	ENSR	**37.41**	33.94	32.09	30.77	26.65	23.79
C.Man	BM3D	**38.29**	**34.18**	31.91	30.49	26.13	23.08
	LSSC	38.24	34.14	31.96	**30.54**	**26.36**	**23.14**
	NCSR	38.17	34.12	31.99	30.48	26.16	22.89
	ENSR	38.26	34.17	**32.03**	30.51	26.19	23.05
Couple	BM3D	**37.52**	**34.04**	**32.11**	**30.76**	**26.46**	**23.51**
	LSSC	37.41	33.96	32.06	30.70	26.31	23.34
	NCSR	37.44	33.94	31.95	30.56	26.21	23.22
	ENSR	**37.52**	33.98	32.00	30.59	26.23	23.31
F.Print	BM3D	36.51	32.46	30.28	28.81	**24.53**	**21.61**
	LSSC	36.71	32.57	30.31	28.78	24.21	21.18
	NCSR	36.81	32.70	30.46	**28.99**	**24.53**	21.29
	ENSR	**36.89**	**32.75**	**30.51**	**28.99**	24.52	21.33
Hill	BM3D	37.13	33.62	31.86	**30.72**	**27.19**	**24.58**
	LSSC	37.16	33.68	31.89	30.71	26.99	24.30
	NCSR	37.17	33.69	31.86	30.61	26.86	24.13
	ENSR	**37.23**	**33.72**	**31.90**	30.64	26.97	24.42
House	BM3D	39.83	36.71	34.94	33.77	29.69	**25.87**
	LSSC	**40.00**	**37.05**	**35.32**	**34.16**	**29.90**	25.63
	NCSR	39.91	36.80	35.11	33.97	29.63	25.65
	ENSR	**40.00**	36.91	35.20	34.04	29.56	25.84
Man	BM3D	37.82	33.98	31.93	30.59	**26.81**	**24.22**
	LSSC	**37.84**	**34.03**	**31.98**	**30.61**	26.72	24.00
	NCSR	37.78	33.96	31.89	30.52	26.60	23.97
	ENSR	**37.84**	33.99	31.92	30.51	26.71	24.18
Peppers	BM3D	38.12	34.68	32.70	31.29	26.68	**23.39**
	LSSC	**38.15**	**34.80**	**32.87**	**31.47**	**26.87**	23.14
	NCSR	38.06	34.66	32.70	31.26	26.53	22.64
	ENSR	38.11	34.69	32.73	31.23	26.67	23.09
Straw	BM3D	35.37	30.92	28.63	27.08	22.41	**19.59**
	LSSC	35.92	31.39	28.95	27.36	**22.67**	19.50
	NCSR	35.87	31.50	29.13	**27.50**	22.48	19.23
	ENSR	**35.96**	**31.56**	**29.16**	**27.50**	22.55	19.42
Average	BM3D	37.76	34.13	32.15	30.80	**26.57**	**23.49**
	LSSC	37.87	34.24	32.23	30.85	26.54	23.29
	NCSR	37.84	34.22	32.21	30.83	26.44	23.14
	ENSR	**37.93**	**34.28**	**32.27**	**30.86**	26.47	23.32

Figure 3: Denoising results on the Hill image ($\sigma = 15$): (a) Noisy image; (b) BM3D (PNSR = 31.86); (c) LSSC (PNSR = 31.89); (d) NCSR (PNSR = 31.86); (e) ENSR (PNSR = 31.90).

Figure 4: Denoising performance comparison on the Lena image ($\sigma = 100$): (a) original image; (b) noisy image; (c) BM3D (PNSR = 25.95); (d) LSSC (PNSR = 25.96); (e) NCSR (PNSR = 25.66); (f) ENSR (PSNR = 25.98).

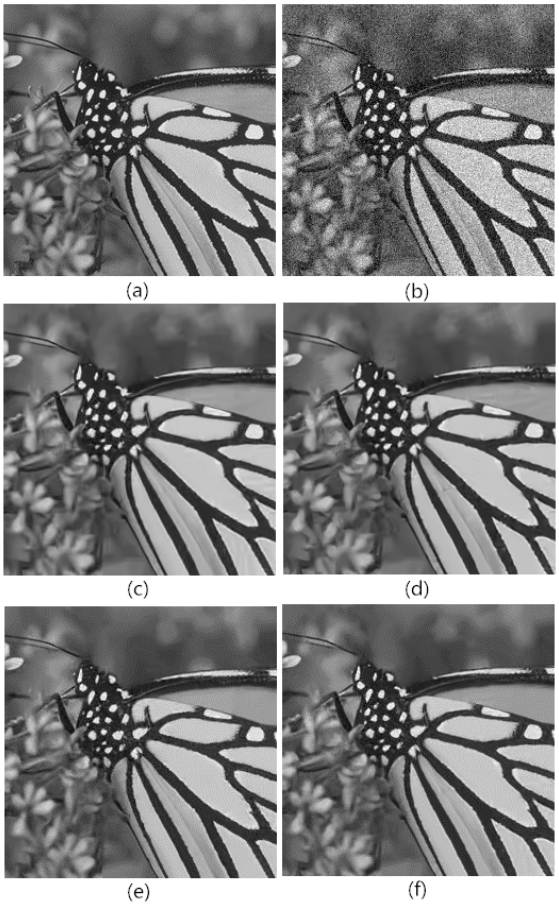

Figure 5: Denoising performance comparison on the Monarch image ($\sigma = 20$): (a) original image; (b) noisy image; (c) BM3D (PNSR = 30.35); (d) LSSC (PNSR = 30.58); (e) NCSR (PNSR = 30.69); (f) ENSR (PNSR = 30.76).

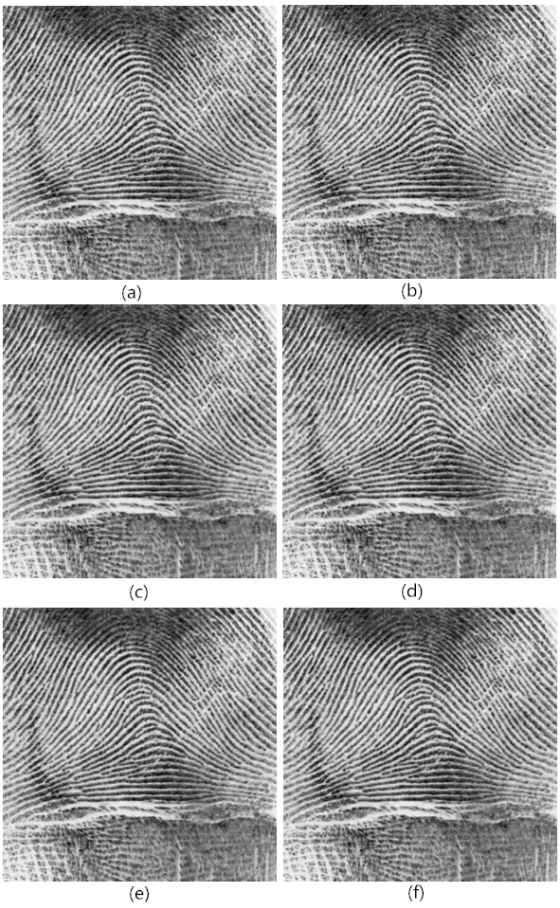

Figure 6: Denoising performance comparison on the Fingerprint image ($\sigma = 15$): (a) original image; (b) noisy image; (c) BM3D (PNSR = 30.28); (d) LSSC (PNSR = 30.31); (e) NCSR (PNSR = 30.46); (f) ENSR (PNSR = 30.51).

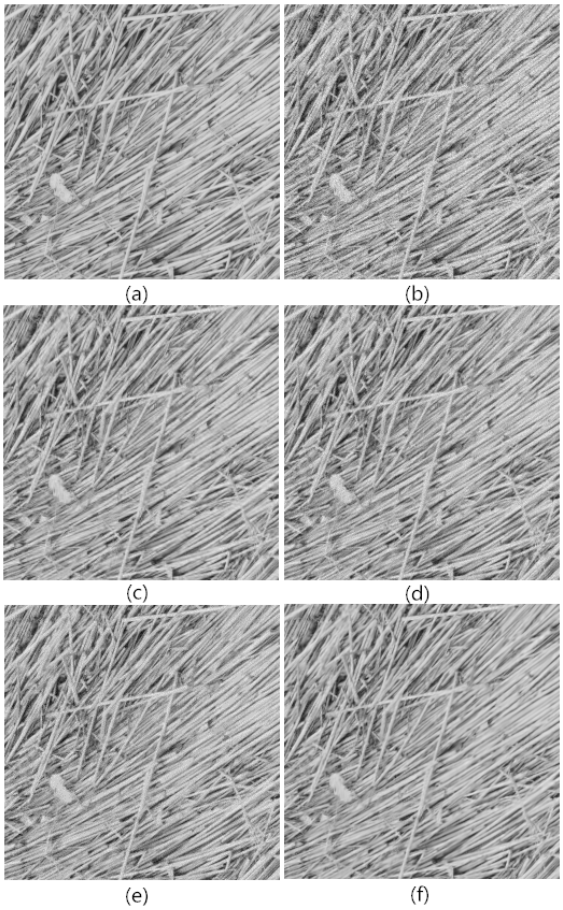

Figure 7: Denoising performance comparison on the Straw image ($\sigma = 10$): (a) original image; (b) noisy image; (c) BM3D (PNSR = 30.92); (d) LSSC (PNSR = 31.39); (e) NCSR (PNSR = 31.50); (f) ENSR (PNSR = 31.56).

Learned Dictionaries, *IEEE Trans. image Process.* vol. 15, no. 12, 2006, pp. 3736-3745.

[3] Y. Romano, M. Elad, Patch-disagreement as a Way to Improve K-SVD Denoising, *IEEE Int. Conf. Acoust. Speech Signal Process.* 2015, pp. 19–14.

[4] J. Mairal, F. Bach, J. Ponce, G. Sapiro, and A. Zisserman, Non-local sparse models for image restoration, *IEEE Int. Conf. Comput. Vis.* 2009, pp. 2272–2279.

[5] W. Dong, L. Zhang, G. Shi, and X. Li, Nonlocally Centralized Sparse Representation for Image Restoration, *IEEE Trans. Image Process.* vol. 22, no. 4, 2013, pp. 1620–1630.

[6] B. Ophir, M. Lustig, and M. Elad, Multi-Scale Dictionary Learning Using Wavelets, *IEEE J. Sel. Topics Signal Process.* vol. 5, no. 5, 2011, pp. 1014–1024.

[7] R. Yan, L. Shao, and Y. Liu, Nonlocal Hierarchical Dictionary Learning Using Wavelets for Image Denoising, *IEEE Trans. Image Process.* vol. 22, no. 12, 2013, pp. 4689–4698.

[8] L. Zhang, W. Dong, D. Zhang, and G. Shi, Two-stage Image Denoising by Principal Component Analysis with Local Pixel Grouping, *Pattern Recognit.* vol. 43, 2010, pp. 1531–1549.

[9] W. Dong, L. Zhang, G. Shi, and X. Wu, Image Deblurring and Superresolution by Adaptive Sparse Domain Selection and Adaptive Regularization, *IEEE Trans. Image Process.* vol. 20, no. 7, 2011, pp. 1838–1857.

[10] K. Dabov, A. Foi, V. Katkovnik, and K. Egiazarian, Image Denoising by Sparse 3-d Transform-domain Collaborative Filtering, *IEEE Trans. Image Process.* vol. 16, no. 8, 2007, pp. 2080–2095.

[11] S. Gu, L. Zhang, W. Zuo, and X. Feng, Weighted Nuclear Norm Minimization with Application to Image Denoising, *IEEE Comput. Vis. Pattern Recognit.* 2014, pp. 2862–2869.

[12] H. Talebi, P. Milanfar, Global Image Denoising, *IEEE Trans. Image Process.* vol. 23, no. 2, 2014, pp. 755–768.

[13] C. Jung, J. Scharcanski, Adaptive Image Denoising and Edge Enhancement in Scale-space Using The Wavelet Transform, *Pattern Recognit. Letters.* vol. 24, no. 7, 2003, pp. 965–971.

[14] C. Ni, Q. Li, and L. Xia, A Novel Method of Infrared Image Denoising and Edge Enhancement, *Signal Process.* vol. 88, no. 6, 2008, pp. 1606–1614.

[15] W. Gao, X. Zhang, L. Yang, and H. Liu, An Improved Sobel Edge Detection, *IEEE Int. Conf. Comput. Sci. Inf. Technol.* vol 5, 2010, pp. 67–71.

[16] P. Qiu, P. Mukherjee, Edge Structure Preserving Image Denoising, *Signal Process.* vol. 90, no. 10, 2010, pp. 2851–2862.

[17] Z. Jiang, Z. Lin, and L. Davis, Learning a Discriminative Dictionary for Sparse Coding via Label Consistent K-SVD, *IEEE Comput. Vis. Pattern Recognit.* 2011, pp. 1697–1704.

[18] I. Daubechies, M. Defriese, and C. DeMol, An iterative thresholding algorithm for linear inverse problems with a sparsity constraint, Commun. Pure Appl. Math. vol. 57, no. 11, 2004, pp. 1413–1457.